

Dynamic Scaling of Two-Dimensional Polar Flocks

Hugues Chaté^{1,2,3} and Alexandre Solon³

¹*Service de Physique de l'Etat Condensé, CEA, CNRS Université Paris-Saclay, CEA-Saclay, 91191 Gif-sur-Yvette, France*

²*Computational Science Research Center, Beijing 100094, China*

³*Sorbonne Université, CNRS, Laboratoire de Physique Théorique de la Matière Condensée, 75005 Paris, France*

(Dated: March 7, 2024)

We propose a hydrodynamic description of the homogeneous ordered phase of polar flocks. Starting from symmetry principles, we construct the appropriate equation for the dynamics of the Goldstone mode associated with the broken rotational symmetry. We then focus on the two-dimensional case considering both “Malthusian flocks” for which the density field is a fast variable that does not enter the hydrodynamic description and “Vicsek flocks” for which it does. In both cases, we argue in favor of scaling relations that allow to compute exactly the scaling exponents, which are found in excellent agreement with previous simulations of the Vicsek model and with the numerical integration of our hydrodynamic equations.

A key result of active matter studies is the possible emergence, in two dimensions, of long-range polar order among locally aligning self-propelled particles [1–5], something unattainable in equilibrium, as proven by the Mermin-Wagner-Hohenberg theorem [6, 7]. However, the properties of the resulting symmetry-broken phase, in particular the temporal and spatial correlations of fluctuations, have remained elusive. In their seminal 1995 paper [2], Toner and Tu (TT) argued that the scaling exponents can be computed exactly in $d = 2$ dimensions, but this argument was later found to fail due to terms that had been missing in the original theory [8]. There was nevertheless hope that the TT95 exponents would still be correct if these new terms were to be renormalized so as to become irrelevant [8]. However, large-scale simulations of the Vicsek model clearly displayed a different scaling [4], calling for a refined theory.

The TT95 exponents were nevertheless thereafter believed to control the scaling of fluctuations of $d = 2$ “Malthusian flocks” within which particles reproduce and die on a short time scale [9], so that, on large scale, the density is effectively constant and drops out of the hydrodynamic description. In a recent paper where we showed that the ordered phase of Malthusian flocks, in the limit of strictly constant density, is in fact metastable [10], we also found exponent values compatible with the TT 1995 predictions.

So far, to our best knowledge, all studies of the ordered phase have started from the “isotropic” Toner-Tu equations (describing the system in all phases) expanded around the ordered state, eliminating the fast degrees of freedom [2, 8, 9, 11–13].

In this Letter, we take a different route, writing directly a generic equation for the dynamics of the hydrodynamic modes of the ordered phase. We first construct the equation for the $d - 1$ Goldstone modes associated with the spontaneously broken continuous symmetry in arbitrary dimension d . We then focus on the $d = 2$ case, considering both the density-less (Malthusian) case and the case relevant to the Vicsek model, when the Goldstone mode

is coupled to a density field. Our approach highlights the symmetries of these equations, which —somewhat surprisingly— were not apparent in previous works. We obtain simpler equations that, importantly, possess a different structure which allows us to derive the scaling exponents in $d = 2$ for both universality classes. Moreover, the numerical integration of our hydrodynamic theory provides a more efficient way to measure the fluctuations of the ordered phase than when using the isotropic equation. We take advantage of this to show that the scaling exponents that we derived agree well with both numerical measurements from our hydrodynamic theory and the large-scale simulations of the Vicsek model of Ref. [4].

We first consider the simpler case of the Malthusian flocks introduced by Toner [9]. Self-propelled particles align locally, but also reproduce and die. As a result of this population dynamics, the density field is a fast mode and thus drops out of the hydrodynamic description, which then only involves a velocity field \mathbf{v} that does *not* obey the incompressibility condition $\nabla \cdot \mathbf{v} = 0$. On the contrary, it can be seen as infinitely compressible [14] and its dynamics are akin to Burgers’ equation with additional alignment terms. In the simple form considered in Ref. [10] that contains the essential terms it reads

$$\partial_t \mathbf{v} + \lambda(\mathbf{v} \cdot \nabla) \mathbf{v} = D \nabla^2 \mathbf{v} + (r - u|\mathbf{v}|^2) \mathbf{v} + \sqrt{2\Delta} \boldsymbol{\xi}, \quad (1)$$

where $\boldsymbol{\xi}$ is a Gaussian white noise field with correlations

$$\langle \xi_\alpha(\mathbf{r}, t) \xi_\beta(\mathbf{r}', t') \rangle = \delta^d(\mathbf{r} - \mathbf{r}') \delta(t - t') \delta_{\alpha\beta}. \quad (2)$$

with Greek indices denoting Cartesian coordinates. At large enough alignment strength r , one can observe a long-range-ordered phase spontaneously breaking the rotational symmetry. Although this phase was found in [10] to be metastable to the nucleation of topological defects, such nucleation, in a large part of the phase diagram, happens very rarely. The scale-free anisotropic correlations of the phase described in [9] can then be observed at will.

The hydrodynamic variable that emerges from the spontaneous symmetry breaking is a direction in space

which we represent by the unit vector field $\mathbf{n}(\mathbf{r}, t)$. Let us construct a dynamical equation for $\mathbf{n}(\mathbf{r}, t)$ that contains all terms allowed by symmetry. As a unit vector, it can only rotate so the dynamics should read

$$\partial_t \mathbf{n} = \mathbf{R} \times \mathbf{n}, \quad (3)$$

with rotation vector \mathbf{R} . Because the symmetry is spontaneously broken, the deterministic part of \mathbf{R} can only come from differences with the local environment. Mathematically, this means that it must be expressed as the divergence of a rank-2 tensor \mathcal{R} . Adding a noise term, the rotation vector then reads

$$R_\alpha = \partial_\beta (\mathcal{R}_{\alpha\beta}) + \sqrt{2\Delta} \xi_\alpha(\mathbf{r}, t) \quad (4)$$

with ξ_α a Gaussian white noise with correlations given by Eq. (2). We then write all possible terms for \mathcal{R} at first order in gradients that respect the $O(d)$ rotational symmetry. They all need to involve the Levi-Civita tensor $\varepsilon_{\alpha\beta\gamma}$ for \mathbf{R} to be an axial vector. We obtain

$$\begin{aligned} \mathcal{R}_{\alpha\beta} = & -\lambda \varepsilon_{\alpha\beta\gamma} n_\gamma \\ & + \varepsilon_{\alpha\gamma\delta} [-D_1(\partial_\beta n_\gamma) n_\delta - D_2(\partial_\gamma n_\beta) n_\delta + D_3(\partial_\gamma n_\delta) n_\beta] \\ & + \varepsilon_{\beta\gamma\delta} [D_4(\partial_\gamma n_\delta) n_\alpha + D_5(\partial_\alpha n_\gamma) n_\delta] \\ & + \varepsilon_{\gamma\alpha\beta} [D_6(\partial_\delta n_\gamma) n_\delta - D_7(\partial_\delta n_\delta) n_\gamma]. \end{aligned} \quad (5)$$

Note that for a passive system \mathbf{n} is not coupled to motion in space and Eq. (5) would then need to obey separately the spatial $O(d)$ symmetry and the $O(n)$ symmetry of \mathbf{n} (with possibly $n \neq d$). This would preclude all terms except D_1 , the only one in which there is no contraction between a spatial derivative and the vector \mathbf{n} .

We now consider specifically the case $d = 2$, parameterizing $\mathbf{n} = (\cos \theta, \sin \theta, 0)$. Eq. (3) becomes $\partial_t \mathbf{n} = \partial_t \theta \mathbf{n}_\perp = R_z \mathbf{n}_\perp$ with $\mathbf{n}_\perp = (-\sin \theta, \cos \theta, 0)$. After computing R_z from Eq. (5), it gives

$$\begin{aligned} \partial_t \theta = & \nabla \cdot [\lambda \mathbf{n}_\perp + D_1 \nabla \theta + (D_3 + D_6) \partial_{||} \theta \mathbf{n} \\ & + (D_2 + D_7) \partial_\perp \theta \mathbf{n}_\perp] + \sqrt{2\Delta} \xi_z \end{aligned} \quad (6)$$

where $\partial_{||} \equiv \mathbf{n} \cdot \nabla$ and $\partial_\perp \equiv \mathbf{n}_\perp \cdot \nabla$. Interestingly, we show in [15] that, adiabatically eliminating the norm of \mathbf{v} (the fast variable) from Eq. (1), the resulting equation for its phase ϕ is not exactly Eq. (6) because it contains diffusion terms which cannot be written as a divergence. However, the dynamics of $\tilde{\phi} = \phi - \alpha \partial_{||} \phi$ for a well-chosen value of α does take the form of Eq. (6). This points to the surprising fact that the Goldstone mode is *not* the phase ϕ of the velocity, as one would naively expect, but, rather, the combination $\tilde{\phi}$.

In the following, we neglect for simplicity the terms with coefficients D_2 , D_3 , D_6 and D_7 . (They lead to anisotropic diffusion terms, which we write explicitly in [15], that are not expected to qualitatively change the large-scale behavior, as will become clear below.) Denoting $D_1 \equiv D$ and $\xi_z \equiv \xi$, Eq. (6) then rewrites as

$$\partial_t \theta + \lambda \partial_{||} \theta = D \nabla^2 \theta + \sqrt{2\Delta} \xi \quad (7)$$

which we believe to be the simplest equation capturing the universal features of Malthusian flocks.

Eq. (7) still possesses $O(2)$ rotational symmetry with θ taking arbitrary values. To investigate the scaling behavior of fluctuations around the ordered state, we assume that the system is globally ordered along the x -axis (corresponding to $\theta = 0$). Shifting to the comoving frame $\mathbf{r} \rightarrow \mathbf{r} - \lambda \mathbf{e}_x$ and expanding the nonlinearities contained in the convective derivative in Eq. (7) yields, at order θ^3 :

$$\partial_t \theta + \lambda_y \partial_y \theta^2 + \lambda_x \partial_x \theta^3 = D_x \partial_x^2 \theta + D_y \partial_y^2 \theta + \sqrt{2\Delta} \xi \quad (8)$$

where we have introduced generic coefficients taking the bare values $\lambda_y = \lambda/2$, $\lambda_x = -\lambda/6$ and $D_x = D_y = D$. An important difference between Eq. (8) and the one obtained in Ref.[9] is the presence here of the λ_x term which we believe was unduly neglected before, being both allowed by symmetry and relevant in the renormalization group (RG) sense. Upon performing a RG step, integrating the short-distance fluctuations over an infinitesimal momentum shell $\Lambda/b \leq |\mathbf{q}| \leq \Lambda$ with $b = 1 + ds$, Λ the ultraviolet cutoff, and rescaling

$$y \rightarrow by, \quad x \rightarrow b^\zeta x, \quad t \rightarrow b^z t, \quad \theta \rightarrow b^\chi \theta, \quad (9)$$

the coefficients of (8) evolve under the RG flow equations

$$\begin{aligned} \frac{d\lambda_x}{ds} &= [2\chi + z - \zeta + \eta_{\lambda_x}] \lambda_x; & \frac{d\lambda_y}{ds} &= [\chi + z - 1 + \eta_{\lambda_y}] \lambda_y; \\ \frac{dD_x}{ds} &= [z - 2\zeta + \eta_{D_x}] D_x; & \frac{dD_y}{ds} &= [z - 2 + \eta_{D_y}] D_y; \\ \frac{d\Delta}{ds} &= \frac{1}{2} [z - 2\chi - 1 - \zeta + 2\eta_\Delta] \Delta \end{aligned} \quad (10)$$

with the anomalous dimensions η_{\dots} coming from ‘‘graphical’’ corrections. Remarkably, the scaling exponents can be determined exactly. First, since the nonlinearities of (8) are derivatives, the noise term does not get graphical corrections, and thus $\eta_\Delta = 0$. Moreover, as we discuss in [15], we believe that the terms coming from the convective derivative also do not receive graphical corrections so that $\eta_{\lambda_x} = \eta_{\lambda_y} = 0$ because of a generalized Galilean invariance. This implies three scaling relations at the infrared fixed point

$$2\chi + z - \zeta = \chi + z - 1 = z - 2\chi - 1 - \zeta = 0 \quad (11)$$

from which one obtains the values of the scaling exponents summarized in Table I. Importantly, the field scales with a negative exponent χ , confirming that the system possesses long-ranged order and that higher-order nonlinearities are irrelevant.

Let us now compare our findings to numerical simulations. To extract the scaling behavior, we compute the Fourier spectrum of equal time correlations $\langle |\theta(\mathbf{q}, t)|^2 \rangle$ which shows the anisotropic scaling [11]

$$\langle |\theta(\mathbf{q}, t)|^2 \rangle \underset{q \rightarrow 0}{\sim} \begin{cases} q_{||}^{-(1+2\chi+\zeta)/\zeta} & \text{for } q_{||} \gg q_\perp^\zeta \\ q_\perp^{-(1+2\chi+\zeta)} & \text{for } q_\perp^\zeta \gg q_{||} \end{cases} \quad (12)$$

TABLE I. Scaling exponents for $d = 2$ Malthusian flocks obtained from our prediction Eq. (11), from the prediction of Toner [9] and from the correlation functions shown in Fig. 1(b-d). The fitting procedure leading our estimates is detailed in [15].

| | This work | Toner 2012 [9] | Numerics |
|---------|-----------|----------------|------------|
| χ | $-1/4$ | $-1/5$ | $-0.25(1)$ |
| ζ | $3/4$ | $3/5$ | $0.75(2)$ |
| z | $5/4$ | $6/5$ | $1.27(3)$ |

Numerical simulations of (7) or (8) are much simpler than those of the isotropic Eq. (1). Indeed, a practical problem in measuring the correlations (12) is that the direction of global order slowly diffuses over time. Strategies to cope with this, discussed in detail in [4], include applying a large enough external field to pin the order along one direction [10] or, for particle systems, considering closed boundary conditions in one spatial direction [4, 16, 17]. All of them affect the dynamics and reduce significantly the range over which unspoiled scaling is observed. Moreover, these methods are imperfect since the direction of order is not strictly pinned and still fluctuates. On the contrary, imposing $\int d\mathbf{r}\xi(\mathbf{r}, t) = 0$ (in practice setting $\xi(\mathbf{q} = 0) = 0$ in Fourier space) at all times when integrating (7) or (8) cancels global rotations and leaves the dynamics of interest intact.

The correlation functions obtained numerically are shown in Fig. 1. All numerical details are given in [15]. In Fig. 1(a), we first compare results obtained in the isotropic Eq. (1) (with an external field applied) and in our Eqs. (7) and (8). We show correlations in the longitudinal direction with $q_{\perp} = 0$ and in the transverse direction with $q_{\parallel} = 0$. We find them nearly identical in all cases except for Eq. (1) in the parallel direction. We believe this discrepancy to come from the fluctuations of the global direction from which, as discussed above, the isotropic equation suffers. In Fig. 1(b-d), we use Eq. (8) which is the most efficient numerically. Fig. 1(c,d) shows the spatial correlations for different noise levels, rescaled by the predicted exponents (for comparison we show the “raw” data and the data rescaled by the exponents of [9] in [15]). The predicted scaling is observed at small enough wave-vector, above a length scale that seems minimal for $\Delta \approx 4$. [18]. The dynamic exponent z is accessed by measuring the space-time correlations $\langle |\theta(\mathbf{q}, \omega)|^2 \rangle$. The width $\Delta\omega$ of the unique propagative mode scales as $q_{\parallel}^{z/\zeta}$ and q_{\perp}^z in the longitudinal and transverse directions respectively (Fig. 1(b)). Fitting the small- q behavior in Fig. 1(b-d), we arrive at the values reported in Table I for the scaling exponents, in very good agreement with the theoretical predictions.

We now turn to the Vicsek universality class, when the Goldstone mode \mathbf{n} is coupled to a conserved scalar field c

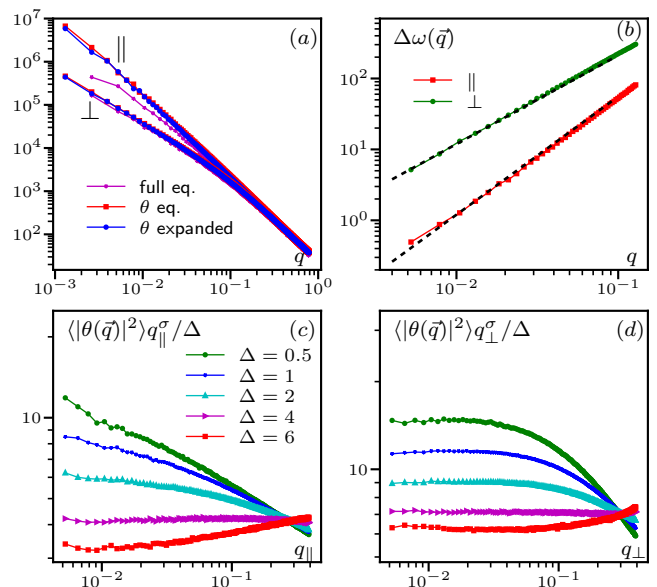


FIG. 1. Correlations of fluctuations in $d = 2$ Malthusian flocks. (a) Static correlation function (12) in the longitudinal direction $\mathbf{q} = (q, 0)$ and perpendicular direction $\mathbf{q} = (0, q)$ measured in the isotropic Eq. (1), the hydrodynamic equation for θ Eq. (7) and its expanded version at order θ^3 , Eq. (8). System size $L = 2400$, $r = u = 1$ for the full equation, $L = 4800$ for the others. $\Delta = 0.5$, $\lambda = D = 1$ for all. (b) Width of the peaks in the ω spectra of $\langle |\theta(\mathbf{q}, \omega)|^2 \rangle$ measured in Eq. (8) ($L = 2400$, $\Delta = 4$, dashed lines are our theoretical predictions). (c-d) Static correlation functions measured in simulations of Eq. (8), rescaled by the predicted exponent $\sigma = (1 + 2\chi + \zeta)/\zeta = 5/3$ in the longitudinal direction (c) and $\sigma = 1 + 2\chi + \zeta = 5/4$ in the transverse direction (d) ($L = 4800$).

representing density fluctuations. The dynamics of \mathbf{n} are still given by Eqs. (3-5), except that now all coefficients depend on density in Eq. (5). In addition, at the same order in gradients and order 2 in c , we have [19]:

$$\partial_t c = -\nabla \cdot [-D_c \nabla c + (v_0 + v_1 c + v_2 c^2 + w_1 \nabla \cdot \mathbf{n} + w_2 \mathbf{n} \cdot \nabla c) \mathbf{n}] \quad (13)$$

Specializing to $d = 2$ and neglecting anisotropic diffusion terms (w_1 and w_2 in (13) and $D_{i>1}$ in (5)), we arrive at

$$\partial_t \theta = \nabla \cdot [(\lambda_0 + \lambda_1 c + \lambda_2 c^2) \mathbf{n}_{\perp} + D \nabla \theta] + \sqrt{2\Delta} \xi \quad (14)$$

where the λ_i coefficients come from expanding $\lambda = \lambda_0 + \lambda_1 c + \lambda_2 c^2$ in Eq. (5). Neglecting the higher-order terms $v_2 c^2 \partial_{\perp} \theta$ and $\lambda_2 c^2 \partial_{\parallel} \theta$, we finally obtain:

$$\begin{aligned} \partial_t c + (v_0 + v_1 c) \partial_{\perp} \theta + v_1 \partial_{\parallel} c + v_2 \partial_{\parallel} c^2 &= D_c \nabla^2 c \quad (15) \\ \partial_t \theta + (\lambda_0 + \lambda_1 c) \partial_{\parallel} \theta &= \lambda_1 \partial_{\perp} c + \lambda_2 \partial_{\perp} c^2 + D \nabla^2 \theta + \sqrt{2\Delta} \xi \quad (16) \end{aligned}$$

where all coefficients are constant. As Eq. (7) did for Malthusian flocks, we believe that Eqs. (15,16) encom-

TABLE II. Scaling exponents for $d = 2$ Vicsek flocks predicted by Eq. (20), in the original Toner and Tu article [2], measured in the Vicsek model by Mahault *et al.* [4], and measured in our simulations of Eqs. (13)–(14).

| | This work | TT 1995 | Mahault <i>et al.</i> | Numerics |
|---------|-----------|---------|-----------------------|------------|
| χ | $-1/3$ | $-1/5$ | $-0.31(2)$ | $-0.34(3)$ |
| ζ | 1 | $3/5$ | $0.95(2)$ | $1.01(4)$ |
| z | $4/3$ | $6/5$ | $1.33(2)$ | $1.30(6)$ |

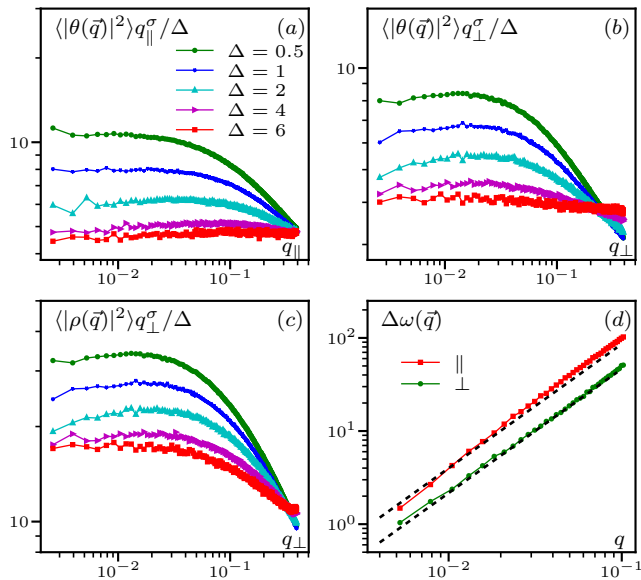


FIG. 2. Correlation of fluctuations in $d = 2$ Vicsek flocks from numerical integration of (15,16). (a–c) Static correlations rescaled by the exponent expected from our prediction $\sigma = 4/3$ ($L = 4800$). (d) Width of the peaks in the dynamic correlation function $\langle |\theta(\mathbf{q}, \omega)|^2 \rangle$ for $\Delta = 4$, $L = 2400$. Parameters $v_0 = 2$, $v_1 = 1$, $\lambda_0 = 0.5$, $\lambda_1 = -0.5$, $\lambda_2 = 0$, $D_c = D = 1$.

pass the universal physics of flocks with conserved density. Again, we show in [15] that the Goldstone mode obtained by eliminating the fast variable from the isotropic Toner-Tu equation is *not* the direction ϕ of the velocity field, as naively expected. This has important consequences for the scaling relations since the nonlinearities in the equation for ϕ are not derivatives [8].

Expanding around the direction of order, assumed to be along \mathbf{e}_x , and introducing a different coefficient for each term we obtain at order 2 in the fields

$$\begin{aligned} \partial_t c + v_1 \partial_x c + v_0 \partial_y \theta + g_x \partial_x \theta^2 + g_y \partial_y (\theta c) \\ + v_2 \partial_x c^2 = D_{cx} \partial_x^2 c + D_{cy} \partial_y^2 c \end{aligned} \quad (17)$$

$$\begin{aligned} \partial_t \theta + \lambda_0 \partial_x \theta - \lambda_1 \partial_y c + h_x \partial_x (\theta c) + h_y \partial_y \theta^2 \\ - \lambda_2 \partial_y c^2 = D_x \partial_x^2 \theta + D_y \partial_y^2 \theta + \sqrt{2\Delta} \xi \end{aligned} \quad (18)$$

with bare values $g_x = -\frac{v_0}{2}$, $g_y = v_1$, $h_x = \lambda_1$, $h_y = \frac{\lambda_0}{2}$, $D_{cx} = D_{cy} = D_c$, $D_x = D_y = D$. Under a RG

step with rescaling (9), and $c \rightarrow b^\chi c$, the coefficients of Eqs. (17,18) flow as

$$\begin{aligned} \frac{dg_x}{ds} &= [\chi + z - \zeta + \eta_{g_x}] g_x; & \frac{dg_y}{ds} &= [\chi + z - 1 + \eta_{g_y}] g_y; \\ \frac{dh_x}{ds} &= [\chi + z - \zeta + \eta_{h_x}] h_x; & \frac{dh_y}{ds} &= [\chi + z - 1 + \eta_{h_y}] h_y; \\ \frac{d\lambda_2}{ds} &= [\chi + z - 1 + \eta_{\lambda_2}] \lambda_2; & \frac{dv_2}{ds} &= [\chi + z - \zeta + \eta_{v_2}] v_2; \\ \frac{d\Delta}{ds} &= \frac{1}{2} [z - 2\chi - 1 - \zeta + 2\eta_{\Delta}] \Delta. \end{aligned} \quad (19)$$

The diffusion coefficients flow similarly as in Eq. (10).

Remarkably, as in the Malthusian case, the scaling exponents can be derived exactly. First, as before, $\eta_{\Delta} = 0$ because all nonlinearities are derivatives. Furthermore, note that the linear drift terms with coefficient $v_{0,1}$ and $\lambda_{0,1}$ in (17,18) are of lower order than those included in Eq. (19), and are thus diverging at a fixed point. These coefficients control the mode structure which contains two normal modes ψ_+ and ψ_- mixing θ and c [11, 20]. As detailed in [15], because the propagators associated to ψ_{\pm} peak at different frequencies with vanishingly small overlap at small wavelength, their dynamics essentially decouple. They then separately obey Galilean invariance, forbidding the renormalization of the quadratic nonlinearities $g_{x,y}$, $h_{x,y}$, v_2 and λ_2 . In the end, none of the terms in Eq. (19) receive graphical corrections so that, at the infrared fixed point, one has the scaling relations

$$\chi + z - \zeta = \chi + z - 1 = z - 2\chi - 1 - \zeta = 0 \quad (20)$$

yielding the exponents reported in Table II.

The predicted values are found to be in agreement with the exponents measured in the Vicsek model [4] also reported in Table II. In addition, we performed numerical simulations of (15,16) for an arbitrarily chosen set of parameters varying the noise intensity Δ . We show in Fig. 2 the same observables as in Fig. 1 with the addition of the density correlations $\langle |c(q_{\parallel} = 0, q_{\perp}, t)|^2 \rangle$ in the transverse direction, expected to scale like the correlations of θ . In the longitudinal direction, the correlations of c have a more complex scaling. It will be the topic of future work to examine these, as well as exploring more broadly the parameter space of Eqs. (15,16). The trend seen in Fig. 2 is the same as for Malthusian flocks: to a good approximation the predicted scaling is reached at large distance after a small-scale regime with a crossover length that is minimal for noise intensity $\Delta \approx 6$. Extracting numerical values by fitting the large scale behavior as detailed in [15] give the numbers reported in Table II, consistent with the predictions.

Conclusion. We have proposed a hydrodynamic theory for the ordered phase of polar flocks based on writing generic equations compatible with the symmetry of these phases. We focused in particular on the $d = 2$ case without density field (Malthusian class) and with density (Vicsek class). In addition to exhibiting clearly the

symmetries, our equations provide an efficient numerical platform to measure correlations of the fluctuations in the ordered phase. Importantly, we have derived exact scaling exponents for the two universality classes in $d = 2$ and found good agreement with the numerical results.

During the writing of this manuscript, two directly relevant preprints have appeared. In the first one [21], Ikeda obtains in the Malthusian case the exponents of [9] reported in Table I, which we have shown to fail, but obtains the same exponent as we do in the Vicsek case, although from different arguments. In [22], Jentsch and Lee tackle the Vicsek case with the non-perturbative renormalization group [23]. They are able to derive exact scaling exponents in arbitrary dimension, different from ours in $d = 2$ (although also compatible with the numerics of [4]), but at the price of neglecting several nonlinearities (g_x , g_y , v_2 , h_x and λ_2 in Eq. (18)). However, these nonlinearities being relevant in the RG sense, we have all reasons to believe that they would break the scaling relations derived in [22].

We believe that our approach opens new possibilities to investigate the symmetry-broken phase of active systems. Future work will be devoted to investigate higher dimensions and other symmetry classes including incompressible flocks and active nematics.

We thank B. Delamotte, J. Horowitz, P. Jentsch, C. F. Lee, B. Mahault, M. Tissier and N. Wschebor for insightful discussions.

-
- [1] T. Vicsek, A. Czirók, E. Ben-Jacob, I. Cohen, and O. Shochet, Novel type of phase transition in a system of self-driven particles, *Physical review letters* **75**, 1226 (1995).
- [2] J. Toner and Y. Tu, Long-range order in a two-dimensional dynamical XY model: how birds fly together, *Physical Review Letters* **75**, 4326 (1995).
- [3] H. Chaté, F. Ginelli, G. Grégoire, and F. Raynaud, Collective motion of self-propelled particles interacting without cohesion, *Physical Review E* **77**, 046113 (2008).
- [4] B. Mahault, F. Ginelli, and H. Chaté, Quantitative assessment of the Toner and Tu theory of polar flocks, *Physical Review Letters* **123**, 218001 (2019), publisher: APS.
- [5] H. Chaté, Dry aligning dilute active matter, *Annual Review of Condensed Matter Physics* **11**, 189 (2020), publisher: Annual Reviews.
- [6] N. D. Mermin and H. Wagner, Absence of ferromagnetism or antiferromagnetism in one-or two-dimensional isotropic Heisenberg models, *Physical Review Letters* **17**, 1133 (1966).
- [7] P. Hohenberg, Existence of long-range order in one and two dimensions, *Physical Review* **158**, 383 (1967).
- [8] J. Toner, Reanalysis of the hydrodynamic theory of fluid, polar-ordered flocks, *Physical Review E* **86**, 031918 (2012).
- [9] J. Toner, Birth, death, and flight: A theory of malthusian flocks, *Physical review letters* **108**, 088102 (2012), publisher: APS.
- [10] M. Besse, H. Chaté, and A. Solon, Metastability of Constant-Density Flocks, *Physical Review Letters* **129**, 268003 (2022), publisher: APS.
- [11] J. Toner and Y. Tu, Flocks, herds, and schools: A quantitative theory of flocking, *Physical review E* **58**, 4828 (1998).
- [12] L. Chen, C. F. Lee, and J. Toner, Universality class for a nonequilibrium state of matter, *Physical Review E* **102**, 022610 (2020), publisher: APS.
- [13] L. Chen, C. F. Lee, and J. Toner, Moving, reproducing, and dying beyond Flatland: Malthusian flocks in dimensions $d > 2$, *Physical Review Letters* **125**, 098003 (2020), publisher: APS.
- [14] L. Di Carlo and M. Scandolo, Evidence of fluctuation-induced first-order phase transition in active matter, *New Journal of Physics* **24**, 123032 (2022), publisher: IOP Publishing.
- [15] See Supplemental Material [url] including Refs.[24–26].
- [16] Y. Tu, J. Toner, and M. Ulm, Sound waves and the absence of Galilean invariance in flocks, *Physical review letters* **80**, 4819 (1998).
- [17] N. Kyriakopoulos, F. Ginelli, and J. Toner, Leading birds by their beaks: the response of flocks to external perturbations, *New Journal of Physics* **18**, 073039 (2016), publisher: IOP Publishing.
- [18] The large crossover scale at small noise explains why we erroneously concluded before [10] that the scaling of fluctuations in Malthusian flocks were consistent with the predictions of Ref. [9].
- [19] We could in principle complement Eq. (13) with a conserved noise term but it is always irrelevant compared to the non-conserved noise on θ .
- [20] D. Geyer, A. Morin, and D. Bartolo, Sounds and hydrodynamics of polar active fluids, *Nature materials* **17**, 789 (2018), publisher: Nature Publishing Group.
- [21] H. Ikeda, How advection stabilize long-range order in two dimensions, *arXiv preprint arXiv:2401.01603* (2024).
- [22] P. Jentsch and C. F. Lee, A new universality class describes Vicsek’s flocking phase in physical dimensions, *arXiv preprint arXiv:2402.01316* (2024).
- [23] B. Delamotte, An introduction to the nonperturbative renormalization group (Springer, 2012) pp. 49–132.
- [24] D. Forster, D. R. Nelson, and M. J. Stephen, Large-distance and long-time properties of a randomly stirred fluid, *Physical Review A* **16**, 732 (1977).
- [25] L. Canet, B. Delamotte, and N. Wschebor, Fully developed isotropic turbulence: Symmetries and exact identities, *Physical Review E* **91**, 053004 (2015), publisher: APS.
- [26] L. Canet, H. Chaté, B. Delamotte, and N. Wschebor, Nonperturbative renormalization group for the Kardar-Parisi-Zhang equation, *Physical review letters* **104**, 150601 (2010).

Supplementary information for “Dynamic Scaling of Two-Dimensional Polar Flocks”

Hugues Chaté^{1,2,3} and Alexandre Solon³

¹*Service de Physique de l'Etat Condensé, CEA, CNRS Université Paris-Saclay, CEA-Saclay, 91191 Gif-sur-Yvette, France*

²*Computational Science Research Center, Beijing 100094, China*

³*Sorbonne Université, CNRS, Laboratoire de Physique Théorique de la Matière Condensée, 75005 Paris, France*

(Dated: March 6, 2024)

I. NUMERICAL DETAILS

The equations are integrated using a semi-spectral algorithm with explicit Euler time-stepping. We use large values of spatial resolution up to $dx = 8$ to speed up the simulations since, as shown in Fig. S1(a,b), this affects only the short-distance physics, leaving the large-scale behavior unchanged.

We show in Fig. S1(c,d) the finite size scaling of the static correlations for a relatively low noise level $\Delta = 1$ for which, on accessible system sizes, the system is not in the scaling regime. As system size increases, we see that the correlations slowly converge toward the expected asymptotic scaling. To reach the asymptotic regime, one would need still much larger system sizes or, alternatively, to tune the noise level in order to minimize the crossover length, as we do in the main text Fig. 1 (c-d) and Fig. 2 (a-c).

Parameters of main text figures:

- Fig. 1 (a): $\Delta = 0.5$, $\lambda = D = 1$, $dx = 4$ and $dt = 0.2$ for all curves. System size $L = 2400$ for the isotropic equation, $L = 4800$ otherwise. As explained in the main text, to compute anisotropic correlation functions, we need to fix the direction of global order along one axis of the simulation box. For the isotropic equation, we thus apply an external field of strength $h = 3 \times 10^{-6}$ along the x -axis.
- Fig. 1 (b): $L = 2400$, $\lambda = D = 1$, $\Delta = 4$, $dx = 8$, $dt = 0.1$.
- Fig. 1 (c-d): $L = 4800$, $\lambda = D = 1$, $dx = 8$, $dt = 0.2/\Delta$.
- Fig. 2: $v_0 = 2$, $v_1 = 1$, $\lambda_0 = 0.5$, $\lambda_1 = -0.5$, $\lambda_2 = 0$, $D_c = D = 1$, $dx = 8$, $dt = 0.05/\Delta$. $L = 4800$ (a-c) or $L = 2400$ (d) and $\Delta = 2$ (d).

II. SCALING EXPONENTS

A. Numerical evaluation

To evaluate numerically the scaling exponents that are reported in Tables I and II (main text), we fit the small q behavior of $\langle |\theta(\vec{q}, t)|^2 \rangle$ in the longitudinal and transverse directions and the width of the peaks of dynamical correlations $\Delta\omega$ in the transverse direction. The fits are done on the data with the noise level $\Delta = 4$ that has a short crossover length. Repeating the fits on the curve with lower noise level gives us an estimate of the error bars. For

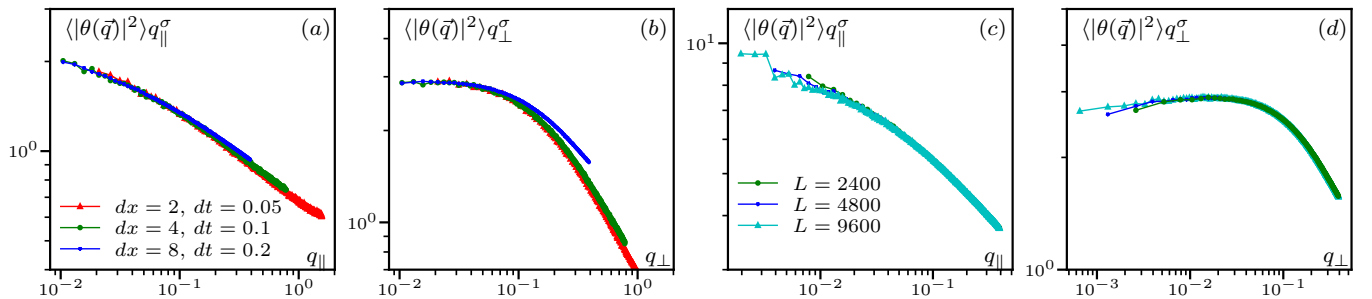


FIG. S1. (a,b): Static correlation functions for varying numerical accuracy dx and dt , rescaled by the predicted scaling exponent. $L = 1200$ for $dx = 2$ and $L = 2400$ for $dx = 4, 8$. (c,d): Static correlations for varying system size. $dx = 8, dt = 0.2$. All panels: simulation of Eq. (8) (main text) with $\lambda = D = \Delta = 1$.

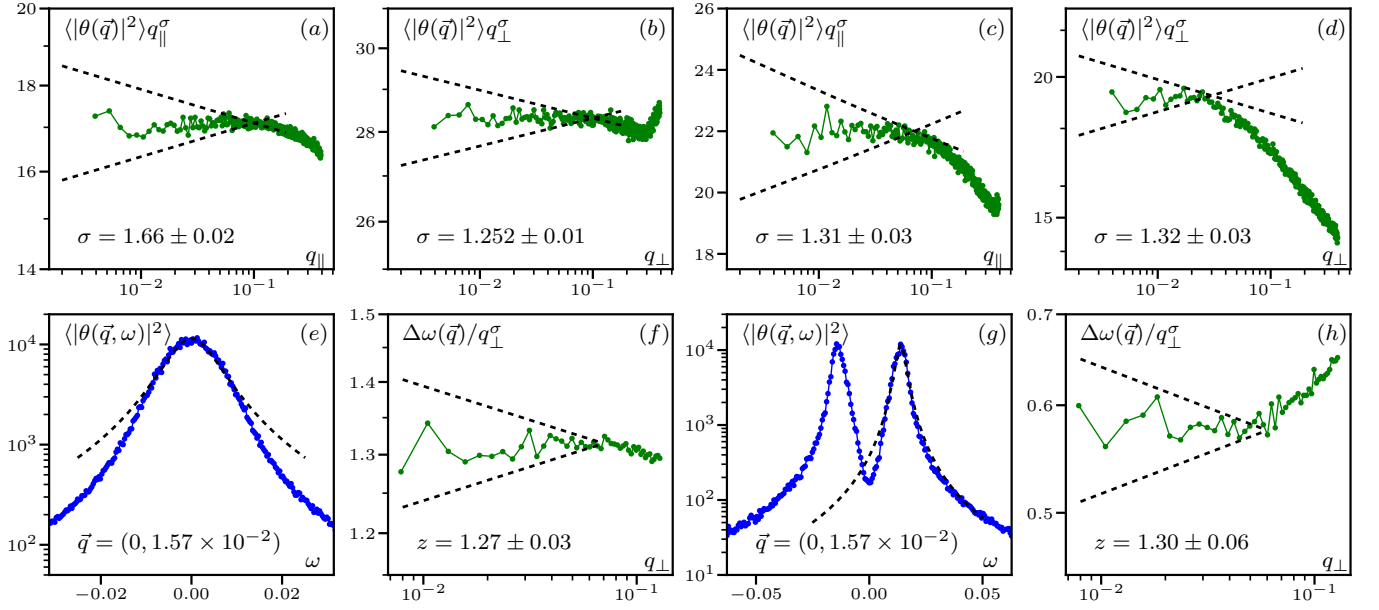


FIG. S2. Numerical evaluation of scaling exponents. Data rescaled by the fitted value of the exponent, indicated on the figure. The black dashed lines materialize the error bars. (a-d): Static correlations in the Malthusian (a,b) and Vicsek (c,d) case. (e,g): Dynamic correlation function from which the width $\Delta\omega$ is extracted by fitting $\langle|\theta(\mathbf{q}, \omega)|^2\rangle = A/(1 + (\omega/\Delta\omega)^2)$ in the Malthusian (e) and Vicsek (g) case. (f,h): Scaling of $\Delta\omega$ in the Malthusian case (f) and Vicsek (h) case.

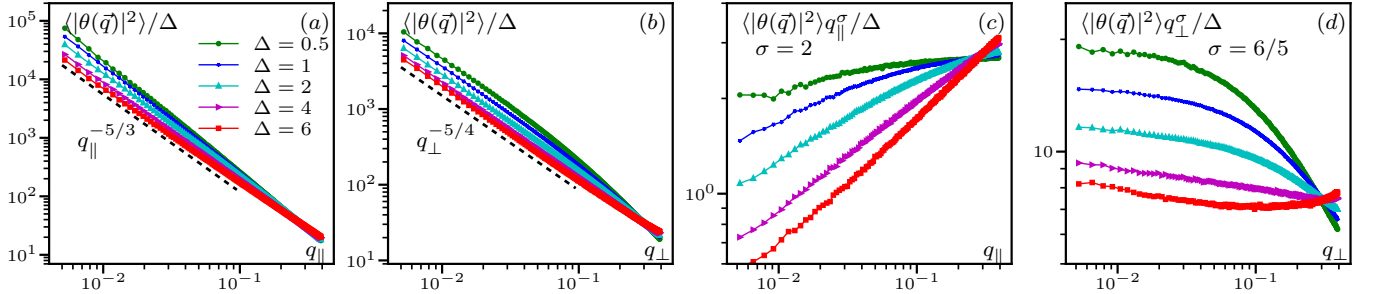


FIG. S3. Static correlations functions in $d = 2$ Malthusian flocks. Same data as in Fig. 1 (c,d) (main text). (a,b): Comparison with the predicted scaling (black dashed line). (c,d): Data rescaled by the exponents predicted in [1].

each fit, we show the data rescaled by the fitted exponent with the error bars in Fig. S2. We see that the estimations of the error bars are consistent with the precision of the data.

B. Non-renormalization arguments

1. Malthusian case

We find that Eq. (8) (main text) is invariant under the transformation

$$\theta'(\mathbf{r}, t) = \theta(\mathbf{r} - \mathbf{r}_c, t) + \theta_0; \quad \partial_t \mathbf{r}_c = \theta_0 \begin{pmatrix} 2\lambda_x \theta \\ \lambda_y \end{pmatrix} \quad (1)$$

for arbitrary transformation parameter θ_0 . When $\lambda_x = 0$, Eq. (1) is a standard Galilean transformation which must be satisfied with the same value of λ_y along the RG flow and thus impose that λ_y does not receive graphical corrections, like in the Burgers [2], Navier-Stokes [3] or KPZ [4] equations.

We expect that the generalized Galilean invariance Eq. (1) lead to the same type of constraint, requiring that both λ_x and λ_y are not graphically corrected. Writing the associated Ward-Takahashi identities is, however, a non-trivial

task since Eq. (1) is a non-linear symmetry, that we defer to future work.

2. Vicsek case

The mode structure generated by the linearized hydrodynamics is well known [5, 6]. It features two propagating sound modes that can be computed from the linearized Eq. (17,18) (main text) in Fourier space and time, for frequency ω and wavevector $\mathbf{q} = (q_x, q_y)$

$$\mathbb{M} \cdot \begin{pmatrix} c(\mathbf{q}, \omega) \\ \theta(\mathbf{q}, \omega) \end{pmatrix} = 0; \quad \mathbb{M} = \begin{pmatrix} i(\omega - q_x v_1) + D_{cx} q_x^2 + D_{cy} q_y^2 & -iq_y v_0 \\ iq_y \lambda_1 & i(\omega - q_x \lambda_0) + D_x q_x^2 + D_y q_y^2 \end{pmatrix} \quad (2)$$

The eigenvalues of \mathbb{M} give two sound modes. At small wavevector $\mathbf{q} = q(\cos \alpha, \sin \alpha)$, their frequency can be written

$$\omega_{\pm} = (c_{\pm}(\alpha)q + O(q^3)) + i\Delta\omega_{\pm} \quad (3)$$

with $\Delta\omega_{\pm} = O(q^2)$ associated with the damping of the wave and the velocities

$$c_{\pm}(\alpha) = \frac{v_1 + \lambda_0}{2} \pm \frac{1}{2} \sqrt{(v_1 - \lambda_0)^2 \cos^2 \alpha - 4v_0 \lambda_1 \sin^2 \alpha}. \quad (4)$$

The associated eigenmodes ψ_{\pm} are linear combinations mixing c and θ . Most importantly, the associated propagators $G_0^{\pm} = (i(\omega - \omega_{\pm}(\mathbf{q})))^{-1}$ are peaked around the frequencies ω_{\pm} with an overlap between the two modes that becomes negligible at small wavenumber since the width of the peaks grows as q_y^z with $z > 1$ [5]. By the same reasoning as explained in [5] (concerning longitudinal and transverse velocities), the normal modes ψ_+ and ψ_- essentially decouple because all terms mixing ψ_+ and ψ_- in their dynamical equation include products of propagators and correlation functions of the two modes that have vanishingly small overlap.

Writing only the lowest-order terms, in Fourier space, the dynamics of ψ_{\pm} then read

$$\psi_{\pm}(\mathbf{q}, \omega) = G_0^{\pm}(\mathbf{q}, \omega) \left[\eta_{\pm}(\mathbf{q}, \omega) + i(a_{\pm} q_x + b_{\pm} q_y) \int d\mathbf{q}' d\omega' \psi_{\pm}(\mathbf{q}', \omega') \psi_{\pm}(\mathbf{q} - \mathbf{q}', \omega - \omega') \right] \quad (5)$$

with $G_0^{\pm} = (i(\omega - \omega_{\pm}(\mathbf{q})))^{-1}$ and coefficients $a_{\pm}(\alpha)$ and $b_{\pm}(\alpha)$ which are combinations of the coefficients of Eq. (17,18) (main text) that can depend on the direction α of the wave-vector but not its amplitude since it would lead to higher order gradient terms. From Eq. (5), one can see that ψ_+ and ψ_- are separately invariant under the Galilean transformation which reads in Fourier space

$$\mathbf{q}' = \mathbf{q}; \quad \omega' = \omega - \mathbf{v} \cdot \mathbf{q}; \quad \psi'_{\pm}(\mathbf{q}', \omega') = \psi_{\pm}(\mathbf{q}, \omega) + \varepsilon \delta^2(\mathbf{q}) \delta(\omega); \quad \mathbf{v} = 2 \begin{pmatrix} a_{\pm} \\ b_{\pm} \end{pmatrix} \varepsilon \quad (6)$$

for any transformation parameter ε . Again, the Galilean invariance prevents the renormalization of the coefficients a_{\pm} and b_{\pm} and thus of the coefficients $g_{x,y}$, $h_{x,y}$, v_2 and λ_2 in Eq. (17,18) (main text).

III. ELIMINATION OF THE FAST DEGREE OF FREEDOM

A. Malthusian flocks

In this section we show how to recover our generic hydrodynamic Eq. (6) (main text) starting from the isotropic ‘‘Toner-Tu’’ equation and integrating the fast degrees of freedom. Expanding Eq. (6) (main text) and putting $D_6 = D_7 = 0$ without loss of generality (they play the same role as D_3 and D_2 respectively in $d = 2$), it reads

$$\partial_t \theta + \lambda \partial_{\parallel} \theta = D_1 \nabla^2 \theta + D_3 \partial_{\parallel} \partial_{\parallel} \theta - D_2 \partial_{\perp} \partial_{\perp} \theta + (D_2 + D_3) \partial_{\parallel} \theta \partial_{\perp} \theta + \sqrt{2\Delta} \xi \quad (7)$$

with Gaussian white noise of unit variance ξ . As shown in the main text, this is the most general equation that should be obeyed by the phase of a Goldstone mode in $d = 2$. We thus expect to recover the same equation starting from the isotropic equation and eliminating the fast degree of freedom.

Let us hence consider the most general equation for a vector field that obeys the rotational $O(d = 2)$ symmetry. We keep terms up to order 2 in gradients and order 3 in the field \mathbf{v} . We thus have a more general version of Eq. (1) (main text)

$$\partial_t \mathbf{v} + \lambda_1 (\mathbf{v} \cdot \nabla) \mathbf{v} + \lambda_2 (\nabla \cdot \mathbf{v}) \mathbf{v} + \lambda_3 \nabla (|\mathbf{v}|^2) = D \nabla^2 \mathbf{v} + D_B \nabla (\nabla \cdot \mathbf{v}) + \alpha (v_0^2 - |\mathbf{v}|^2) \mathbf{v} + \sqrt{2\Delta} \xi, \quad (8)$$

with Gaussian white noise of unit variance $\boldsymbol{\xi}$ as in the main text. Let us parameterize the velocity vector as $\mathbf{v} = v(\mathbf{r}, t)\mathbf{n}(\phi(\mathbf{r}, t))$ with $\mathbf{n}(\phi) = (\cos \phi, \sin \phi)$ the unit vector pointing in direction ϕ . We can rewrite Eq. (8) for the two variables v and ϕ , using that $\partial_t \mathbf{v} = \partial_t v \mathbf{n} + v \partial_t \phi \mathbf{n}_\perp$ with $\mathbf{n}_\perp = (-\sin \phi, \cos \phi)$, projecting on \mathbf{n} and \mathbf{n}_\perp gives

$$\partial_t v + \lambda_1 v \partial_{\parallel} v + \lambda_2 (v \partial_{\parallel} v + v^2 \partial_{\perp} \phi) + 2\lambda_3 v \partial_{\parallel} v = D (\nabla^2 v - v(\nabla \phi)^2) + D_B \partial_{\parallel} (v \partial_{\perp} \phi + \partial_{\parallel} v) + \alpha (v_0^2 - v^2) v + \sqrt{2\tilde{\Delta}} \xi_{\parallel} \quad (9)$$

$$\partial_t \phi + \lambda_1 v \partial_{\parallel} \phi + 2\lambda_3 \partial_{\perp} v = D \left(\nabla^2 \phi + \frac{2\nabla v \cdot \nabla \phi}{v} \right) + \frac{D_B}{v} \partial_{\perp} (v \partial_{\perp} \phi + \partial_{\parallel} v) + \sqrt{2\tilde{\Delta}} \xi_{\perp} / v \quad (10)$$

where $\partial_{\parallel} = \mathbf{n}_{\parallel} \cdot \nabla$, $\partial_{\perp} = \mathbf{n}_{\perp} \cdot \nabla$ and ξ_{\parallel} and ξ_{\perp} are the two components of $\boldsymbol{\xi}$ in Eq. (8).

The norm of the velocity is a fast variable which relaxes in a time of order $(\alpha v_0^2)^{-1}$. We can eliminate it, formally by doing an expansion at large α . We want to retain terms only up to order ∇^2 in the equation for ϕ . We thus keep the terms up to order ∇ for v ,

$$v \approx v_0 - \frac{\lambda_2}{2\alpha} \partial_{\perp} \phi. \quad (11)$$

Inserting in Eq. (10), we obtain

$$\partial_t \phi + \lambda \partial_{\parallel} \phi = D \nabla^2 \phi + D_{\perp} \partial_{\perp} \partial_{\perp} \phi + D_{\times} \partial_{\parallel} \phi \partial_{\perp} \phi + \sqrt{2\tilde{\Delta}} \xi_{\perp} \quad (12)$$

with $\lambda = v_0 \lambda_1$, $D_{\perp} = D_B + \lambda_2 \lambda_3 / \alpha$, $D_{\times} = \lambda_1 \lambda_2 / (2\alpha)$ and $\tilde{\Delta} = \Delta / v_0^2$.

Interestingly, Eq. (12) does not have exactly the same form as Eq. (7) because the coefficients of the diffusion terms have a different structure: the terms D_{\perp} and D_{\times} differ from the three diffusion terms with coefficient $D_{2,3}$ in Eq. (7). However, we can easily recover the structure of Eq. (7) by considering the combination $\tilde{\phi} = \phi - \alpha \partial_{\parallel} \phi$. At the same order in gradient, it follows that

$$\partial_t \tilde{\phi} + \lambda \partial_{\parallel} \tilde{\phi} = D \nabla^2 \tilde{\phi} + D_{\perp} \partial_{\perp} \partial_{\perp} \tilde{\phi} + (D_{\times} - \alpha \lambda) \partial_{\parallel} \tilde{\phi} \partial_{\perp} \tilde{\phi} + \sqrt{2\tilde{\Delta}} \xi_{\perp} \quad (13)$$

Choosing $\alpha = (D_{\perp} + D_{\times}) / \lambda$, Eq. (13) is exactly Eq. (7) upon identifying $D_1 = D$, $D_2 = -D_{\perp}$ and $D_3 = 0$. The fact that we had to consider a different variable $\tilde{\phi}$ to make the identification suggests that the phase ϕ of the velocity vector is not the correct Goldstone mode to consider in the ordered phase. Note that this change of variable makes sense only for an active system in which the direction of order couples to spatial directions.

B. Compressible flocks

Let us repeat the same procedure in the case when the velocity is coupled to the density field. We consider the Toner-Tu equations

$$\begin{aligned} \partial_t \mathbf{v} + \lambda_1 (\mathbf{v} \cdot \nabla) \mathbf{v} + \lambda_2 (\nabla \cdot \mathbf{v}) \mathbf{v} + \lambda_3 \nabla (|\mathbf{v}|^2) &= -\nabla P(\rho) + D \nabla^2 \mathbf{v} + D_B \nabla (\nabla \cdot \mathbf{v}) + \alpha (v_0^2 - |\mathbf{v}|^2) \mathbf{v} + \sqrt{2\tilde{\Delta}} \boldsymbol{\xi} \\ \partial_t \rho + \nabla \cdot (\rho \mathbf{v}) &= 0 \end{aligned} \quad (14)$$

with pressure $P(\rho) = \sigma_1 \rho + \sigma_2 \rho^2$. As before we parameterize the velocity vector as $\mathbf{v} = v(\mathbf{r}, t)\mathbf{n}(\phi(\mathbf{r}, t))$. We also expand around the homogeneous density $\rho(\mathbf{r}, t) = \rho_0 + c(\mathbf{r}, t)$. In principle all coefficients in Eq. (14) depend on density. For simplicity, we retain only that of $\lambda_1 = \lambda_{10} + \lambda_{1c} c$, which is enough to generate the important nonlinearities [7]. We follow the same procedure as in the previous section to eliminate the norm of the velocity vector. Solving the equation for v at order $O(v, c, \nabla)$ now gives

$$v \approx v_0 - \frac{\lambda_2}{2\alpha} \partial_{\perp} \phi - \frac{\sigma}{2v_0^2 \alpha} \partial_{\parallel} c \quad (15)$$

with $\sigma = \sigma_1 + 2\rho_0 \sigma_2$. The remaining equations for ϕ and c then read

$$\begin{aligned} \partial_t \phi + \lambda \partial_{\parallel} \phi + g c \partial_{\parallel} \phi + \tilde{\sigma} \partial_{\perp} c &= -\tilde{\sigma} \partial_{\perp} c^2 + D \nabla^2 \phi + D_{\perp} \partial_{\perp} \partial_{\perp} \phi + D_{\times} \partial_{\parallel} \phi \partial_{\perp} \phi \\ &+ D_{\phi c} (\partial_{\parallel} \phi \partial_{\parallel} c - \partial_{\perp} \phi \partial_{\perp} c) + D_{cc} \partial_{\perp} c \partial_{\parallel} c + \sqrt{2\tilde{\Delta}} \xi_{\perp} \end{aligned} \quad (16)$$

$$\partial_t c + \nabla \cdot [(\rho_0 v_0 + v_0 c + w_1 \partial_{\perp} \phi + w_2 \partial_{\parallel} c) \mathbf{n}] = 0 \quad (17)$$

with coefficients

$$\lambda = v_0 \lambda_{10}; \quad g = v_0 \lambda_{1c}; \quad \tilde{\sigma} = \frac{\sigma}{v_0}; \quad \tilde{\sigma}_2 = \frac{\sigma_2}{v_0}; \quad D_{\perp} = D_B + \frac{\lambda_2 \lambda_3}{\alpha}; \quad D_{\times} = \frac{\lambda_{10} \lambda_2}{2\alpha}; \quad (18)$$

$$D_{\phi c} = \frac{\lambda_{10} \sigma}{2v_0^2 \alpha}; \quad D_{cc} = -\frac{\sigma^2}{2v_0^4 \alpha}; \quad \tilde{\Delta} = \frac{\Delta}{v_0^2}; \quad w_1 = -\frac{\lambda_2 \rho_0}{2\alpha}; \quad w_2 = -\frac{\sigma \rho_0}{2v_0^2 \alpha}; \quad (19)$$

We want to compare with the generic hydrodynamic equations for a Goldstone mode coupled to a conserved density field, as constructed in the main text. Compared to the Malthusian case, all parameters can depend on density. Starting from Eq. (6) (main text) (again with $D_6 = D_7 = 0$ without loss of generality) we consider coefficients $\lambda = \lambda^{(0)} + \lambda^{(1)}c + \lambda^{(2)}c^2 + \lambda^{(3)}\partial_{\parallel}c$, $D_i = D_i^{(0)} + D_i^{(1)}c$ with $i = 1, 2, 3$ (we depart from the notation of the main text to avoid confusion with the coefficients of the Toner-Tu equation). We obtain the analog of Eq. (7) when density is taken into account

$$\partial_t \theta + \lambda^{(0)} \partial_{\parallel} \theta - \lambda^{(1)} \partial_{\perp} c + \lambda^{(1)} c \partial_{\parallel} \theta = \lambda^{(2)} \partial_{\perp} c^2 + D_1^{(0)} \nabla^2 \theta + D_3^{(0)} \partial_{\parallel} \partial_{\parallel} \theta - D_2^{(0)} \partial_{\perp} \partial_{\perp} \theta + (D_2^{(0)} + D_3^{(0)}) \partial_{\parallel} \theta \partial_{\perp} \theta \quad (20)$$

$$+ D_1^{(1)} \nabla c \cdot \nabla \theta + D_3^{(1)} \partial_{\parallel} c \partial_{\parallel} \theta + D_2^{(1)} \partial_{\perp} c \partial_{\perp} \theta + \lambda^{(3)} \partial_{\parallel} c \partial_{\perp} c + \sqrt{2\Delta} \xi \quad (21)$$

As in the Malthusian case, we find that Eq. (16) obtained from the Toner-Tu equation differs from the expected hydrodynamic Eq. (20). They differ, as before, in the structure of the diffusion terms $D_2^{(0)}$ and $D_3^{(0)}$ but also, more crucially, in the structure of the $\lambda^{(1)}$ terms. Indeed, the terms $\partial_{\perp} c$ and $c \partial_{\parallel} \theta$ have the same coefficient $\lambda^{(1)}$ in Eq. (20) (because of the underlying gradient structure) while the two terms have different coefficients in Eq. (16). This again indicates that ϕ is not a Goldstone mode and thus not the correct variable to consider in a hydrodynamic theory. One should instead consider

$$\tilde{\phi} = \phi - \alpha \partial_{\parallel} \phi - \beta c \partial_{\parallel} \phi; \quad \alpha = \frac{D_{\perp} + D_{\times}}{\lambda}; \quad \beta = \frac{g - \tilde{\sigma}}{\lambda} \quad (22)$$

which dynamics follows Eq. (20) and is thus a Goldstone mode. Note that there is no problem for the c equation since the same terms are found in both Eq. (17) and in the hydrodynamic theory Eq. (15) (main text), as expected since c is obviously a conserved quantity and thus a proper slow mode on which to build a hydrodynamic theory.

C. Hydrodynamic theory with the naive choice of variables

For concreteness, let us explore what happens when taking Eq. (16,17) as our hydrodynamic theory, as is done *e.g.* in [7]. Expanding around $\phi = 0$ in powers of ϕ leads, compared to Eq. (17,18) (main text), to more general terms $h_{x,1} c \partial_x \phi + h_{x,2} \phi \partial_x c$ with $h_{x,1} \neq h_{x,2}$ in general, instead of the derivative term $h_x \partial_x (c\theta)$. We simulated this equation with the same parameters as in Fig. 2 (main text) and varying $h_{x,2}$. As shown in Fig. S4, we find that only for $h_{x,2} = h_{x,1}$ do we observe the expected scale-free fluctuations. For $h_{x,2} < h_{x,1}$ we find that the equation is numerically unstable while for $h_{x,2} > h_{x,1}$, the system shows short-ranged correlations, signaled by the small- q plateau in the correlation functions. The plateau is reached beyond a crossover length that diverges as $h_{x,2} \rightarrow h_{x,1}$. These results are consistent with the fact that ϕ is not a slow variable, except in the special case $h_{x,2} = h_{x,1}$.

-
- [1] J. Toner, Physical review letters **108**, 088102 (2012), publisher: APS.
 - [2] D. Forster, D. R. Nelson, and M. J. Stephen, Physical Review A **16**, 732 (1977).
 - [3] L. Canet, B. Delamotte, and N. Wschebor, Physical Review E **91**, 053004 (2015), publisher: APS.
 - [4] L. Canet, H. Chaté, B. Delamotte, and N. Wschebor, Physical review letters **104**, 150601 (2010).
 - [5] J. Toner and Y. Tu, Physical review E **58**, 4828 (1998).
 - [6] D. Geyer, A. Morin, and D. Bartolo, Nature materials **17**, 789 (2018), publisher: Nature Publishing Group.
 - [7] J. Toner, Physical Review E **86**, 031918 (2012).

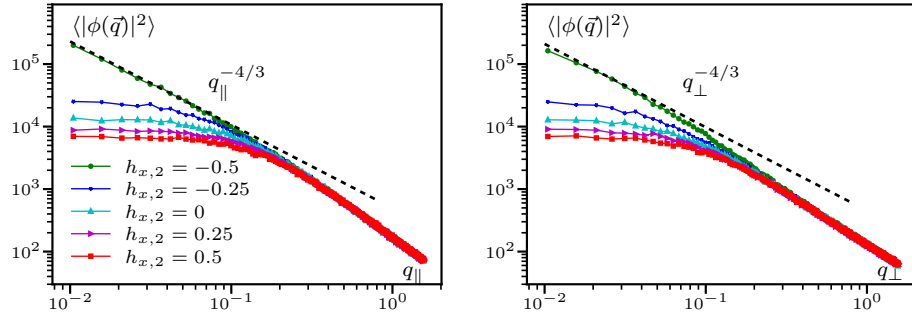


FIG. S4. Correlation of fluctuations from numerical integration of the equations for c and ϕ with a non-derivative term $h_{x,1}c\partial_x\phi + h_{x,2}\phi\partial_x c$ in the dynamics of ϕ , as described in Sec. III C. We use the same parameter values as in Fig. 2 (main text) $v_0 = 2$, $v_1 = 1$, $\lambda_0 = 0.5$, $\lambda_1 = -0.5$, $\lambda_2 = 0$, $D_c = D = 1$ with $h_{x,1} = \lambda_1 = -0.5$. For all $h_{x,2} < h_{x,1}$, we have found that the system is numerically unstable. $L = 1200$, $dx = 2$, $dt = 0.05$.